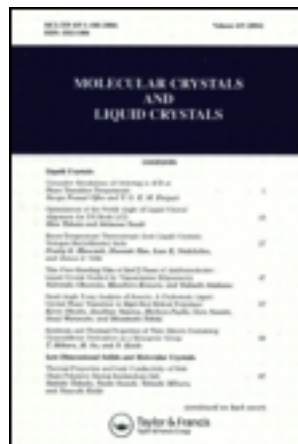


This article was downloaded by: [Moskow State Univ Bibliote]

On: 15 April 2012, At: 12:10

Publisher: Taylor & Francis

Informa Ltd Registered in England and Wales Registered Number: 1072954 Registered office: Mortimer House, 37-41 Mortimer Street, London W1T 3JH, UK



## Molecular Crystals and Liquid Crystals

Publication details, including instructions for authors and subscription information:

<http://www.tandfonline.com/loi/gmcl20>

### Polymer Network Morphology and Electro-Optical Properties of Electrothermal Switchable Bistable Polymer-Stabilized Cholesteric Texture Light Shutters with Various Chiral Dopant Concentrations

Hao-Hsun Liang<sup>a</sup>, Po-Hsiang Wang<sup>a</sup>, Cheng-Che Wu<sup>a</sup>, Shuo-Chan Hsu<sup>a</sup> & Jiunn-Yih Lee<sup>a</sup>

<sup>a</sup> Department of Materials Science and Engineering, National Taiwan University of Science and Technology, Taipei, Taiwan, Republic of China

Available online: 27 Dec 2011

To cite this article: Hao-Hsun Liang, Po-Hsiang Wang, Cheng-Che Wu, Shuo-Chan Hsu & Jiunn-Yih Lee (2012): Polymer Network Morphology and Electro-Optical Properties of Electrothermal Switchable Bistable Polymer-Stabilized Cholesteric Texture Light Shutters with Various Chiral Dopant Concentrations, *Molecular Crystals and Liquid Crystals*, 552:1, 111-122

To link to this article: <http://dx.doi.org/10.1080/15421406.2011.606012>

PLEASE SCROLL DOWN FOR ARTICLE

Full terms and conditions of use: <http://www.tandfonline.com/page/terms-and-conditions>

This article may be used for research, teaching, and private study purposes. Any substantial or systematic reproduction, redistribution, reselling, loan, sub-licensing, systematic supply, or distribution in any form to anyone is expressly forbidden.

The publisher does not give any warranty express or implied or make any representation that the contents will be complete or accurate or up to date. The accuracy of any instructions, formulae, and drug doses should be independently verified with primary sources. The publisher shall not be liable for any loss, actions, claims, proceedings, demand, or costs or damages whatsoever or howsoever caused arising directly or indirectly in connection with or arising out of the use of this material.

# Polymer Network Morphology and Electro-Optical Properties of Electrothermal Switchable Bistable Polymer-Stabilized Cholesteric Texture Light Shutters with Various Chiral Dopant Concentrations

HAO-HSUN LIANG,\* PO-HSIANG WANG, CHENG-CHE WU,  
SHUO-CHAN HSU, AND JUINN-YIH LEE

Department of Materials Science and Engineering, National Taiwan University  
of Science and Technology, Taipei, Taiwan, Republic of China

*Electrothermal switchable bistable (ETSB) polymer-stabilized cholesteric (Ch) texture (PSCT) light shutters (ETSB-PSCT) with various chiral dopant concentrations were fabricated and the effects of the chiral dopant concentrations on the morphology of polymer network and electro-optical performances of ETSB-PSCT were studied. As the chiral dopant concentrations increased, higher monomer concentrations were required to maintain the unwound homeotropic texture of the cholesteric liquid crystals for the fabrication of the ETSB-PSCT. Electro-optical measurements indicated that as the chiral dopant concentration increased, the contrast ratio of the scattering and transparent states of the ETSB-PSCT increased. In particular, 12 wt% ETSB-PSCT exhibited optimum electro-optical performance. We also discovered that 3 wt% ETSB-PSCT possessed two stable optical states at zero field, under two different rates of the removal of the voltage. This development has paved the way for the possible fabrication of electro-electro switchable bistable PSCT (EESB-PSCT) light shutters.*

**Keywords** Bistable light shutter; chiral dopant concentration; monomer concentration; polymer-stabilized cholesteric texture

## 1. Introduction

In recent years, optical devices combining the respective merits of liquid crystals (LCs) and polymers have become the subject of extensive research and widely employed in applications. For example, polymer-dispersed liquid crystals (PDLCs) [1–6], with a high monomer content, and polymer-stabilized cholesteric (Ch) texture (PSCT) [7–15], with a low monomer content, are the most widely used light shutters that do not require a polarizer. In the PSCT normal mode, the polymers are vertically aligned to the substrate, with the aligning effect tending to stabilize the unwound structure, as opposed to the intermolecular forces between Ch LC molecules, which tend to form the helical structure. The competition between these two forces is heavily dependent on the polymer concentration and the chiral

---

\*Address correspondence to Mr. Hao-Hsun Liang, Department of Materials Science and Engineering, National Taiwan University of Science and Technology, Taipei, Taiwan, Republic of China. Tel./Fax: +886-2-27376519. E-mail: D9504402@mail.ntust.edu.tw

dopant concentration. At zero electric field, the chiral-polymer diagram of the normal mode PSCT can be broken down into three regions according to the increasing concentrations of the polymers: (1) unstable, (2) stable and scattering, and (3) stable and clear [16]. In Region (1), the polymer concentration is too low, with the result that the focal conic (FC) texture cannot be completely stabilized. Therefore, the scattering level of the PSCT cell is low, and the reproducibility of the electro-optical performance is poor. Region (2) encompasses the operational range of the PSCT normal mode. At this point, the FC texture is stabilized, and the scattering level of the cell and the reproducibility of the electro-optical performance are both excellent. In Region (3), the exceedingly high polymer concentration leads to the stabilization of the homeotropic (H) texture after ultraviolet (UV) curing. At this point, the cell remains in a transparent state.

Recently, the discovery that the use of annealing treatment can successfully reduce the aligning effects of the polymer networks means that PSCT cells in Region (3) can also possess stable scattering FC texture at zero electric field [17,18]. As a result, one can maintain two optical states without the need for an additional voltage, and fabricate energy-efficient bistable light shutters [18]. Due to the bistable characteristics, the contrast ratio between the bright and dark states has become the most important evaluation parameter. The dark state of this bistable light shutter is generated by the FC texture of the Ch LC, and the scattering performance of the FC texture is heavily dependent on the length of the pitch. The appropriate chiral dopant concentration will result in the optimized contrast ratio between the bright and dark states of the electrothermal switchable bistable (ETSB) PSCT (ETSB-PSCT) light shutter.

In this article, we altered the chiral dopant concentration to find the matching monomer concentration, and applied a sufficiently large voltage during the UV curing process to effect the transition to the H texture, thereby creating polymer networks vertically aligned to the cell surface to fabricate ETSB-PSCT light shutters. At zero field, the aligning effects of the polymer networks were sufficiently strong to maintain the transparent H texture, as shown in Fig. 1(a). With annealing treatment, we reduced the aligning effects of the polymer networks and reverted back to the scattering FC texture due to the intermolecular interactions of the Ch LC, as shown in Fig. 1(b). We studied the effects of different chiral dopant concentrations on the morphology of polymer networks and electro-optical properties, such as driving voltage, contrast ratio, etc., of the ETSB-PSCT light shutters to determine the optimum conditions for fabrication.

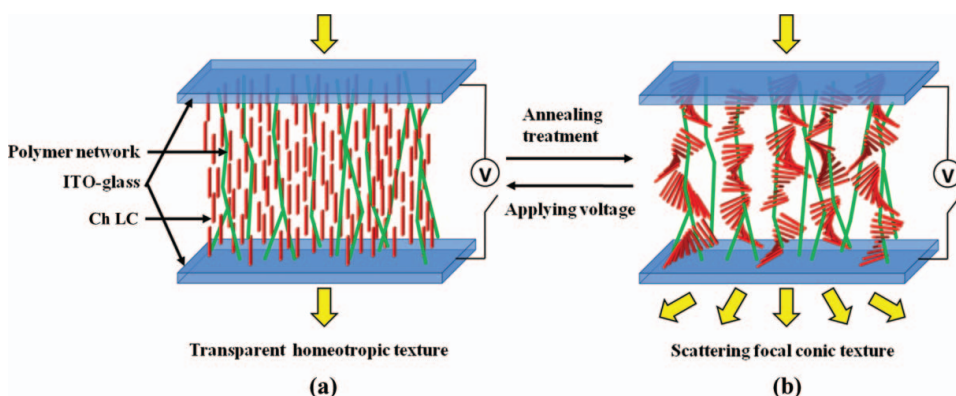


**Figure 1.** Schematic diagram of the operation of the ETSB-PSCT light shutter (Color figure available online).

## 2. Experiment

The Ch LC used was a mixture of a nematic LC ( $\Delta\epsilon=13.03$ ,  $\Delta n=0.24$ , from Daily Polymer) and a chiral dopant S811 (from Merck). The pitch length of the PSCT cells was controlled by adjusting the concentration of S811. The weight concentrations of S811 were 3%–15%, which generated a pitch of about 3.0–0.6  $\mu\text{m}$  from the helical twisting power equation  $\text{HTP} = 1/\text{PC}$ , where P is the pitch and C is the concentration of the chiral dopant. The mesogenic diacrylate monomer RM257 (from Merck) was dissolved in the Ch LC mixture at 1.5–6.0 wt%. A small amount (0.4 wt%) of the photoinitiator Irgacure 651 (from Ciba Additive) was added to the mixture to initiate the polymerization of the monomer RM257. After UV irradiation, the resulting anisotropic polymer network structure was expected to assume the orientation order of the Ch LC. The 16- $\mu\text{m}$  ETSB-PSCT cells, which were controlled by the dispersion of cylindrical glass spacers, consisted of two transparent indium tin oxide (ITO)-coated glass substrates and were filled with the Ch LC/monomer mixtures. The filled cells were irradiated by UV light at 10  $\text{mW cm}^{-2}$  and a curing time of approximately 1 h for photopolymerization at room temperature. An AC voltage was applied to the cells during polymerization at the frequency of 1 kHz.

Observations of the morphology of the polymer networks of the PSCT cells were carried out with scanning electron microscopy (SEM, Leica LEO 420). For the top view, the PSCT cells were separated with caution; after which the ITO substrate with PSCT material was dipped in *n*-hexane for 24 h at room temperature. The ITO substrate with the polymer networks was subsequently dried in vacuum. This way the Ch LC was extracted and only the polymer networks were left on the substrate. After the ITO substrate with the polymer networks was sputtered with a thin layer of gold, the polymer networks of the PSCT cells were observed under the SEM. For the side view, the SEM sample preparation processes were the same as aforementioned except for the cell separation. The pure Ch LC and PSCT textures were studied with polarizing optical microscopy (POM, OLYMPUS Optical Co., Ltd., Models BHSP-2, BX-51) in conjunction with a temperature controller (Mettler Toledo FP 90).

For the electro-optical properties, an He–Ne laser (632.8 nm, 10 mW) incident at normal to the sample was employed as the light source. The light transmitted through the sample was collected by a photodiode detector. The AC electric field was supplied by a function generator in conjunction with a high-voltage amplifier. All AC voltage electro-optical measurements were carried out at the frequency of 1 kHz.

## 3. Results and Discussion

Due to the anisotropic nature of the LC, the environment for the monomers was anisotropic during the polymerization. Coupled to the aligning effects of the LC on the monomers, anisotropic polymer networks were formed [19]. In the ETSB-PSCT system, the monomers began polymerization under the H texture, forming polymer networks vertically aligned to the cell substrates. When the voltage was removed, since the aligning effects of the polymer network were greater than the intermolecular interactions among the LC molecules, the unwound H texture was stabilized. We employed the SEM to ascertain the morphology of the polymer networks. Figure 2 shows the SEM photographs of the side view of the ETSB-PSCT cells. The upper and lower portions of the photograph are the ITO-glass substrates. From the figure, one can observe that the polymer networks formed a fiber-like structure and were vertically aligned to the cell substrates, with two ends attached to the cell substrates. As the monomer concentration increased from 2.5 wt% to 6.0 wt%,

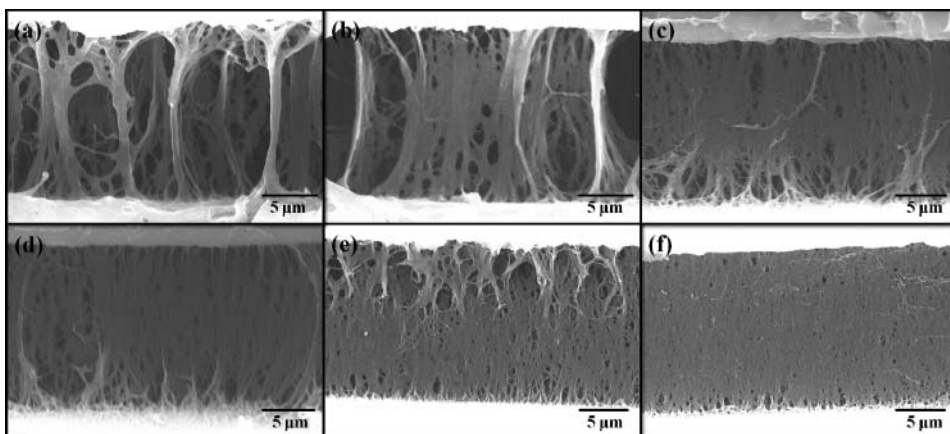


**Figure 2.** Side-view SEM photographs of homeotropically aligned polymer networks with different monomer concentrations: (a) 2.5, (b) 3.4, (c) 4.0, (d) 4.6, (e) 4.7, and (f) 5.1 wt%.

the polymer strand density increased, resulting in the formation of a more closely packed polymer structure with smaller average void sizes. At the monomer concentration of 6.0 wt%, a film-like morphology was formed. Since the strength of the aligning effects of the polymer was proportional to the polymer network density, and the polymer network density was determined by the monomer concentration, higher monomer concentrations would be able to maintain the Ch LC with shorter pitches. In other words, the Ch LC with greater chiral dopant concentrations would exist in the unwound state.

Figure 3 shows the SEM photographs for monomer concentrations of 2.5 and 4.0 wt%, respectively. Other than Figs 3(a) and (d), which are the top-view SEM photographs, the rest are SEM photographs obtained by tilting the normal of the substrate  $40^\circ$  away from the incident electron beam. In the top-view SEM photographs, the honeycomb morphology

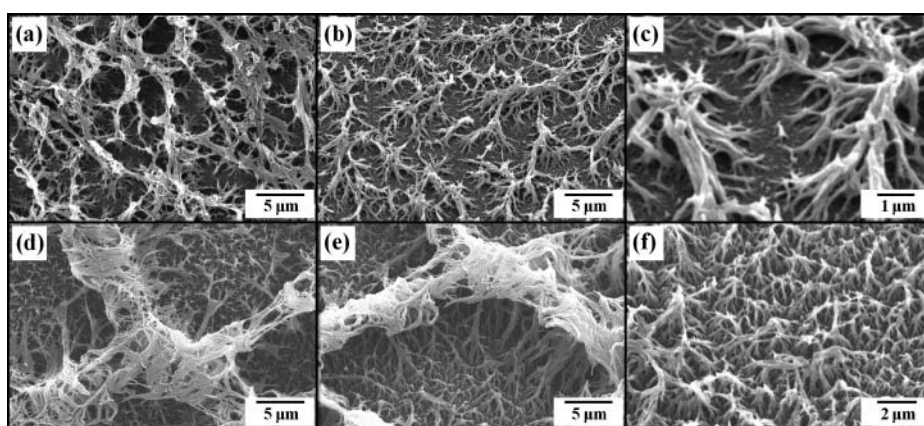


**Figure 3.** SEM photographs of homeotropically aligned polymer networks. The monomer concentration (wt%), the tilt angle ( $^\circ$ ) of the normal of the substrate away from the incident electron beam, and the magnifications were (a) 2.5X, 0 $^\circ$ , and 4000 $\times$ ; (b) 2.5 $\times$ , 40 $^\circ$ , and 4000 $\times$ ; (c) 2.5 $\times$ , 40 $^\circ$ , and 15,000 $\times$ ; (d) 4.0 $\times$ , 0 $^\circ$ , and 4000 $\times$ ; (e) 4.0 $\times$ , 40 $^\circ$ , and 4000 $\times$ ; and (f) 4.0 $\times$ , 40 $^\circ$ , and 8000 $\times$ .

of the polymer networks observed resulted from the retraction of the polymer fibers in the direction parallel to the substrate during solvent evaporation. In particular, in Fig. 3(d), the higher polymer density led to regions where the polymer strands resulting from the retraction became entangled and appeared larger than those of the 2.5 wt% concentration, under observation at the same magnification. After tilting the substrate by  $40^\circ$ , one can also clearly see that one end of the polymer networks was tightly attached to the substrate like the roots of a tree, as shown in Figs 3(b) and (e), the same as the results from Fig. 2. As for the other end of the polymer, the fractures resulting from the cell separation can be clearly observed under higher magnifications as in Fig. 3(c). In Fig. 3(f), the higher monomer concentration meant that in comparison with Fig. 3(b), it was almost impossible to discern the substrate from Fig. 3(b).

Figure 4 shows the VT characteristics for PSCT cells with different monomer concentrations and chiral dopant concentrations of 3, 5, 8, 10, 12, and 15 wt% respectively. Each of the cells was measured at  $30^\circ\text{C}$  after the annealing treatment at  $90^\circ\text{C}$ . In each chiral dopant concentration, we showed the electro-optical performances of three different monomer concentrations. The monomer concentrations corresponding to the Ch LC with different chiral dopant concentrations could be classified into three distinct ranges: minute, moderate, and excessive. When the monomer concentration dropped to the minute range, the aligning effects of the polymer networks were not strong enough and unable to maintain the Ch LC in the unwound H texture after UV curing. The latter thus exhibited a scattering FC texture, which transformed into a transparent H texture with an increase in the applied voltage. At this point, the orientation of the LC was parallel with the polymer networks. As the voltage was gradually removed, the aligning effects of the polymer networks affected the Ch LC back to the FC texture, resulting in the hysteresis phenomenon during the FC-H transition. Since the monomer concentration was higher than that of the traditional PSCT normal mode, the transmittance was unable to return to its initial low value even when the voltage was gradually reduced to zero. Overall, within this range, the interactions among the Ch LC were stronger than the aligning effects of the polymer networks at zero electric field. While the transmittance values varied, the differences were not significant.

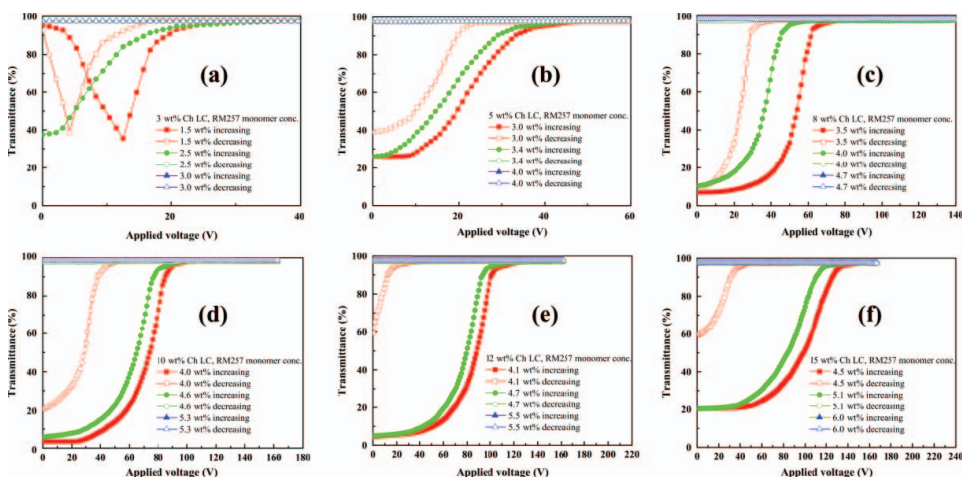


**Figure 4.** Transmittance as a function of the applied voltage for PSCT cells with various monomer concentrations. The chiral dopant concentrations were (a) 3, (b) 5, (c) 8, (d) 10, (e) 12, and (f) 15 wt% (Color figure available online).

When the monomer concentration increased to the moderate range, annealing treatment was first applied to reduce the aligning effects of the polymer networks to achieve an FC texture with almost identical scattering to the cells in the minute range. A voltage was applied to achieve the H texture before being gradually reduced to zero. Since the aligning effects of the polymer networks were stronger than the interactions between the Ch LC, they sufficed for maintaining this unwound state, which exhibited the stable transparent H texture. There existed bistable bright and dark states in the cells within this concentration range in the absence of an applied voltage, and also the operating range of a bistable light shutter. In a bistable light shutter, the anisotropic polymers possess a tendency to unwind the helical structure of the Ch LC. On the other hand, the LC molecules possess a tendency to maintain the helical structure. If the helical structure is unwound, the relationship for the elastic energy is given by [18]

$$f_{elas} = \frac{1}{2} k_{22} \left( \frac{2\pi}{p} \right)^2, \quad (1)$$

where  $k_{22}$  is the twist elastic constant. From this equation, we know that as the chiral dopant concentration increased, the pitch became shorter, and the tendency to maintain the helical structure became stronger. At this point, a higher polymer concentration was required to maintain the unwound H texture, from the 2.5 wt% required for the 3 wt% Ch LC in Fig. 4(a) to the 5.1 wt% required for the 15 wt% Ch LC in Fig. 4(f). In summary, the polymers formed within this concentration range shared a characteristic: after the unwinding of the Ch LC, the polymer networks were just sufficient to anchor the LC. However, the converse was true when the temperature rose.

When the monomer concentration continued to rise to the excessive range, we observed that in the annealing process, when the temperature transitioned from the isotropic phase into the mesophase, the polymer networks immediately anchored the LC and maintained the H texture throughout the cooling process. Overall, the aligning forces of the polymer networks were too strong within this concentration range, and neither the removal of the electric field nor annealing treatment would make it possible to attain the FC texture. The cells continued to exhibit a stable H texture with high transmittance. For the 1.5 wt% cell in Fig. 4(a), because of the excessively low monomer concentration and longer pitch, a mostly transparent P texture was obtained after the annealing treatment. As the voltage increased, the P texture transformed into the FC texture and H texture, and reverted back to the P texture after the complete removal of the electric field.

Next, we compared the driving voltage and the contrast ratio of ETBS-PSCT light shutters with different chiral dopant concentrations. For the driving voltage, the polymers in the cell could be considered as impurities, and the relation between the driving voltage of pure Ch LC and the pitch is given by

$$E_d = \frac{2\pi}{p} \sqrt{\frac{\pi k_{22}}{\Delta\epsilon}}, \quad (2)$$

where  $\Delta\epsilon$  is the anisotropic dielectric constant. From the above equation, we know that  $E_d \propto 1/p \propto C_c$ . Combining the aforementioned two factors, one can deduce that the 15 wt% ETBS-PSCT light shutter, with the highest chiral dopant concentration and monomer concentration, will naturally exhibit the maximum drive voltage of 55 V, as shown in Fig. 5. Figure 6 shows the relationship between different chiral dopant concentrations and the maximum and minimum transmittance as well as the maximum value of contrast ratio for the ETBS-PSCT cells. From the figure, one can observe that ETBS-PSCT cells for

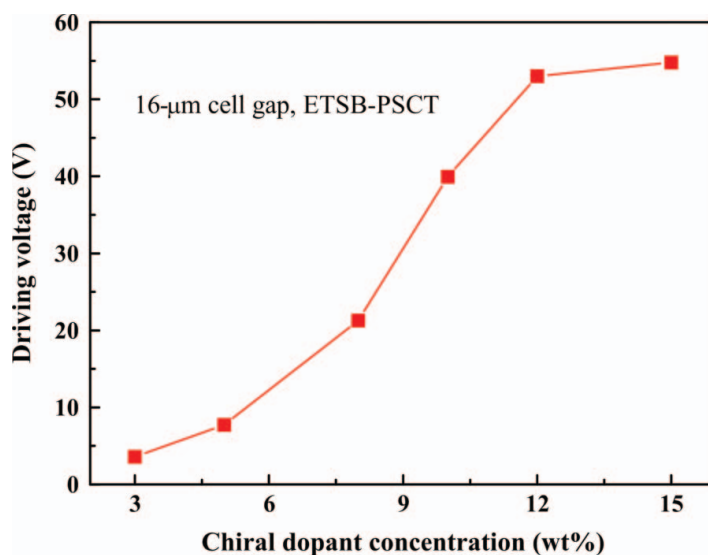


**Figure 5.** Dependence of the driving voltage of the ETSB-PSCT light shutters on various chiral dopant concentrations (Color figure available online).

each chiral dopant concentration exhibited almost the identical bright state, above 97%, while the performance of the dark state decreased and then increased with increasing chiral dopant concentrations. This result determined the differences in the contrast ratio. The chiral dopant concentration directly affected the FC domain size. From Fig. 7, which shows the dark-state POM microphotographs for ETSB-PSCT cells with different chiral dopant concentrations, one can observe that as the concentration increased, the FC domain reduced in size. However, when the FC domain was too big or too small, the scattering capacity would be weakened. The 12 wt% FC domain possessed the best scattering ability

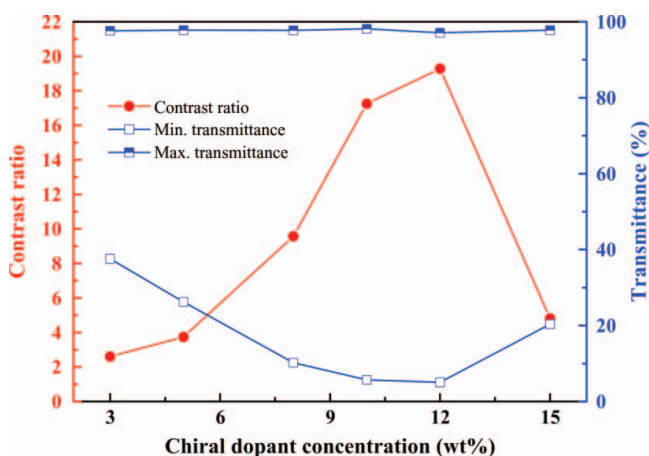


**Figure 6.** Dependence of the maximum and minimum transmittance values and the contrast ratios of the ETSB-PSCT light shutters on various chiral dopant concentrations (Color figure available online).

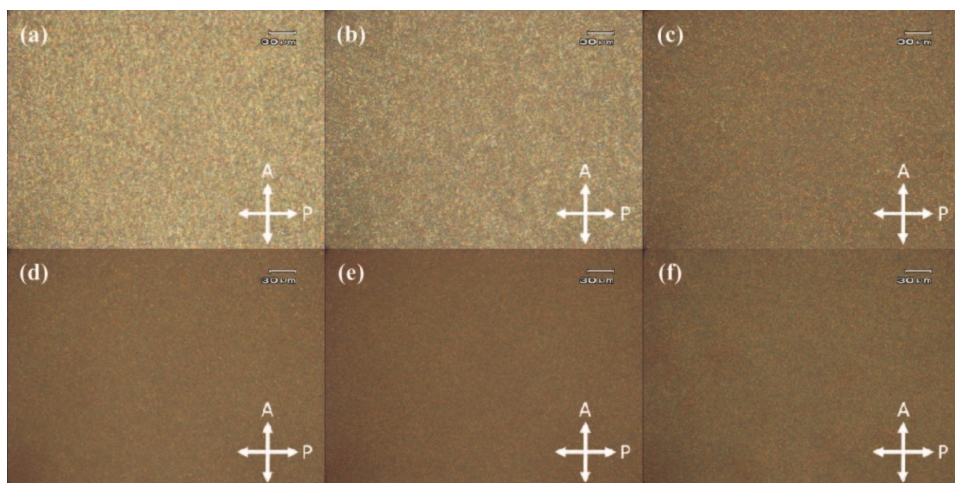
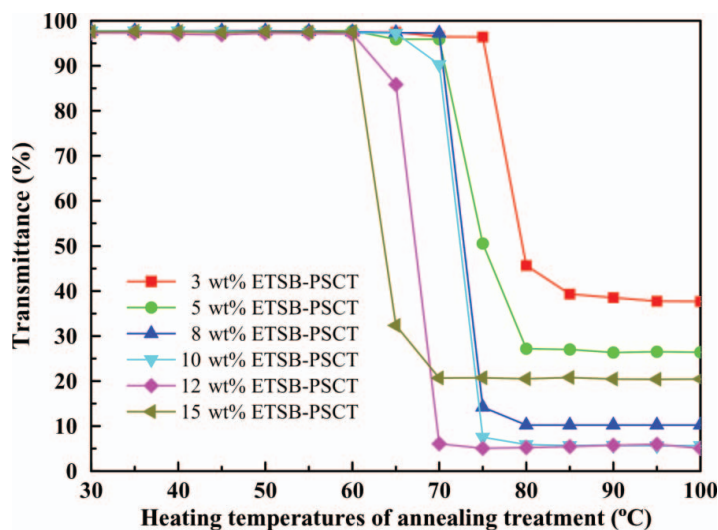


**Figure 7.** The microphotographs of the scattering state of ETSB-PSCT light shutters with various chiral dopant concentrations under crossed polarizers: (a) 3, (b) 5, (c) 8, (d) 10, (e) 12, and (f) 15 wt% (Color figure available online).

for incident light, resulting in a reflection point at this concentration for the trend in the contrast, with a contrast of about 20.

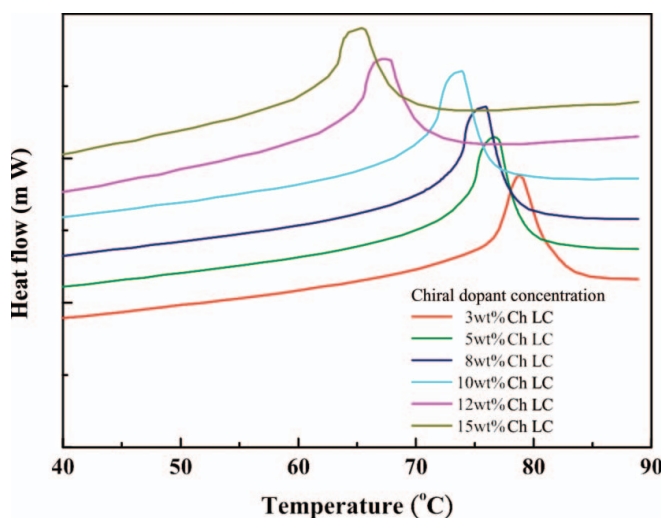
The annealing treatment of the ETSB-PSCT reduced the aligning effects of the polymer networks and led to a reversion back to the stable dark state. When studying the relationship between the transmittance values of ETSB-PSCT cells with different concentrations and the heating temperatures of the annealing treatment, we observed that the cholesteric–isotropic (Ch–Iso) transition temperature for Ch LC of various concentrations was an important parameter. When the monomer concentration was minute, the aligning effects of the polymer networks thus formed were weak. Therefore, when the annealing temperature was lower than the phase transition temperature, a small portion of the H texture would transform into the FC texture, with the transmittance value dropping to its lowest value. When the monomer concentration was moderate, the aligning effects of the polymer networks were stronger, meaning that the original voltage-driven transparent H texture could be maintained almost to the point when transition to the FC texture took place only after the annealing temperature reached the phase transition temperature. Naturally, the transmittance dropped to its minimum value. The results are shown in Fig. 8. In the figure, each data point represents the transmittance measured by heating the PSCT to the temperature indicated by its  $x$ -coordinate, followed by cooling to 30°C at a cooling rate of 10°C min<sup>−1</sup>, after which the measurement was taken.

Figure 9 shows the differential scanning calorimetry (DSC) thermograms for Ch LC with different chiral dopant concentrations. As the chiral dopant concentration increased, the phase transition temperature  $T_{\text{Ch-Iso}}$  dropped from 78°C to 65°C, in correspondence with the rapid drop in the transmittance values of ETSB-PSCT cells in Fig. 8. This indicated that ETSB-PSCT cells with higher chiral dopant concentrations, such as 15 wt% ETSB-PSCT, would require less thermal energy to switch from the bright to the dark state, under the same annealing treatment conditions. However, when the monomer concentration was excessive, the cell remained in a high transmittance state.



**Figure 8.** Dependence of the transmittance of ETSB-PSCT light shutters with various chiral dopant concentrations on the heating temperatures of the annealing treatment (Color figure available online).

The dark and bright states displayed in the ETSB-PSCT can be affected by annealing treatment or the gradual application followed by the removal of a voltage. We further attempted to speed up the removal of the voltage to achieve more energy-efficient driving. Our results indicated that the bright states of almost all the ETSB-PSCT cells were independent of the rate of the removal of the voltage, with the exception of the 3 wt% ETSB-PSCT cell. The rest of the ETSB-PSCT cells could all retain bistable characteristics at a faster rate. Figures 10(a) and (b) show the dynamic transmittance response curve for the 3 wt%



**Figure 9.** The DSC thermograms of pure Ch LC with various chiral dopant concentrations displaying sharp peaks for the Ch-Iso transition on the heating scan

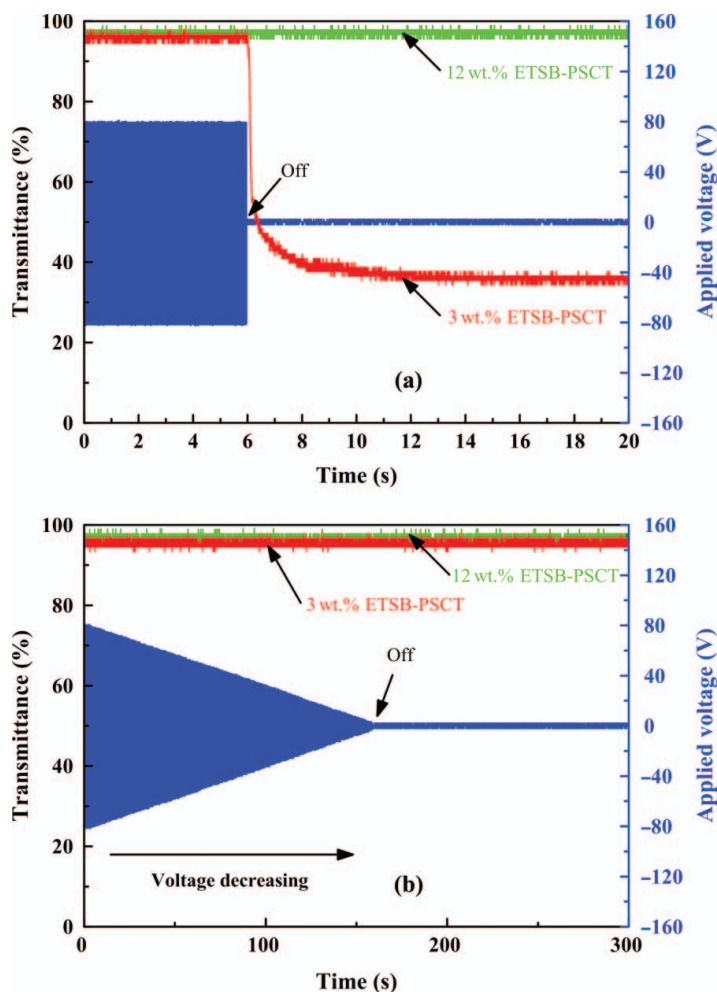


**Figure 10.** Dynamic transmittance response curves of the 3 wt% and 12 wt% ETSB-PSCT light shutters. The rates of the removal of the voltage were (a) 160 and (b) 1 V s<sup>-1</sup> (Color figure available online).

and 12 wt% ETSB-PSCT cells under two different modes of voltage removal: gradual and abrupt. From the figure, one can see that the 12 wt% ETSB-PSCT cell maintained a stable bright state under the two different modes. On the other hand, the 3 wt% ETSB-PSCT cell was unable to maintain the bright state under the abrupt removal of the voltage, and instead exhibited the same stable dark state with the same transmittance value as that obtained by annealing treatment. The reason for this might be that the degree of the reversion of the LC molecules to the helical structure was proportional to the rate of the removal of the voltage, and the monomer concentration of the 3 wt% ETSB-PSCT was right at the boundary of the minute and moderate regions. This resulted in the aligning effects of the polymer networks being just able to maintain the H texture at slower rates of the removal of the voltage. However, when the voltage helping to maintain the H texture was abruptly turned off, the LC reverted to the helical structure, whose strength meant that the aligning effects were unable to maintain the H texture, which transformed into the FC texture.

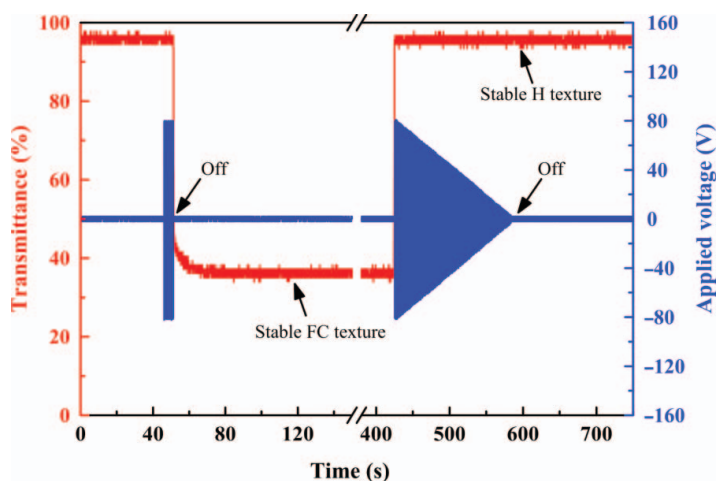


**Figure 11.** Dynamic transmittance response curves of the 3 wt% ETSB-PSCT light shutter under different rates of the removal of the voltage. The square voltage pulse was 160 V at 1 kHz (Color figure available online).

This result suggested yet another approach to achieve bistable characteristics by altering the rate of the removal of the voltage, as shown in Fig. 11. The 3 wt% ETSB-PSCT was initially in the bright state, and a stable dark state was obtained with an abrupt removal of the voltage. Subsequently, a gradual application of the voltage restored the cell to the stable bright state.

Figure 12(a) shows a photograph of the 12 wt% ETSB-PSCT light shutter at zero field and room temperature after the annealing treatment to the FC texture. The light shutter was scattering and blocked the scene behind. Figure 12(b) shows a photograph of the light

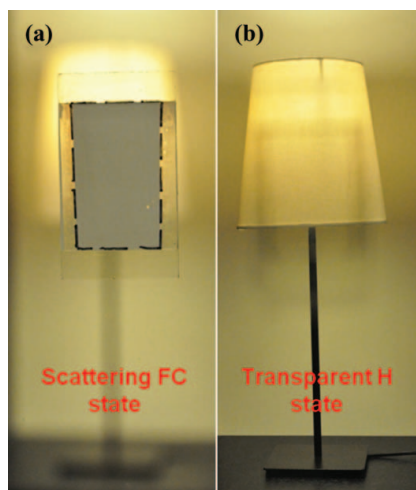


**Figure 12.** Photographs of the 12 wt% ETSB-PSCT light shutter at zero voltage: (a) in the scattering FC texture and (b) in the transparent H texture

shutter at zero field and room temperature after electrically switched to the H texture. The shutter was transparent and the scene behind was clearly visible.

#### 4. Conclusions

In this study, we categorized the monomer concentrations corresponding to different chiral dopant concentrations into three distinct ranges for a detailed examination of the optical performances. ETSB-PSCT light shutters fabricated by using monomer concentrations in the moderate region transformed into the stable scattering FC texture after the annealing treatment, and could be electrically switched to a stable transparent H texture. Comparing the optical and electrical performances of ETSB-PSCT light shutters with different chiral dopant concentrations, we observed that the 12 wt% ETSB-PSCT possessed the highest contrast ratio, thus requiring less thermal and electrical energy to switch between the bright and dark states, and was thus the most optimum for fabrication. In addition, we found that 3 wt% ETSB-PSCT possessed two optical states at different rates of the removal of the voltage, which paved the way for a new approach for fabricating electro-electro switchable bistable PSCT (EESB-PSCT) light shutters.

#### References

- [1] Weiss, R. A., & Ober, C. K. (1990). *Liquid-Crystalline Polymers*, American Chemical Society: Washington, DC.
- [2] Drzaic, P. S. (1995). *Liquid Crystal Dispersions*, World Scientific: Singapore.
- [3] Doane, J. W., Vaz, N. A., Wu, B.-G., & Žumer, S. (1986). *Appl. Phys. Lett.*, **48**, 269.
- [4] Sutherland, R. L., Tondiglia, V. P., Natarajan, L. V., Bunning, T. J., & Adams, W. W. (1994). *Appl. Phys. Lett.*, **64**, 1074.
- [5] Kłosowicz, S. J., & Aleksander, M. (2004). *Opto-Electron. Rev.*, **12**, 305.
- [6] Montgomery, G. P., & Vaz, N. A. (1987). *Appl. Opt.*, **26**, 738.
- [7] Yang, D.-K., Chien, L.-C., & Doane, J. W. (1992). *Appl. Phys. Lett.*, **60**, 3102.
- [8] Yang, D.-K., West, J. L., & Doane, J. W. (1994). *Appl. Phys. Lett.*, **76**, 1331.
- [9] Dierking, I., Kosbar, L. L., Afzali-Ardakani, A., Lowe, A. C., & Held, G. A. (1997). *J. Appl. Phys.*, **81**, 3007.
- [10] Dierking, I., Kosbar, L. L., Lowe, A. C., & Held, G. A. (1998). *Liq. Cryst.*, **24**, 397.
- [11] Dierking, I., Kosbar, L. L., Lowe, A. C., & Held, G. A. (1998). *Liq. Cryst.*, **24**, 387.
- [12] Dierking, I. (2000). *Adv. Mater.*, **12**, 167.
- [13] Wu, S.-T., & Yang, D.-K. (2001). *Reflective Liquid Crystal Displays*, Wiley: New York.
- [14] Ren, H., & Wu, S.-T. (2002). *J. Appl. Phys.*, **92**, 797.
- [15] Huang, C.-Y., Chih, Y. S., & Ke, S. W. (2007). *Appl. Phys. B*, **86**, 123.
- [16] Crawford, G. P., & Zumer, S. (1996). *Liquid Crystals in Complex Geometries Formed by Polymer and Porous Networks*, Taylor & Francis: London.
- [17] Tien, C.-J., & Huang, C.-Y. (2008). *Jpn. J. Appl. Phys.*, **47**, 8515.
- [18] Bao, R., Liu, C.-M., & Yang, D.-K. (2009). *Appl. Phys. Express*, **2**, 112401.
- [19] Ma, R.-Q., & Yang, D.-K. (2000). *Phys. Rev. Lett.*, **61**, 1567.